Coupling of hydrodynamics and quasiparticle motion in collective modes of superfluid trapped Fermi gases

M. Urban

Coupling of hydrodynamics and quasiparticle motion in collective modes of superfluid trapped Fermi gases

Michael Urban

Institut de Physique Nucléaire, CNRS and Univ. Paris-Sud, 91406 Orsay Cédex, France

At finite temperature, the hydrodynamic collective modes of superfluid trapped Fermi gases are coupled to the motion of the normal component, which in the BCS limit behaves like a collisionless normal Fermi gas. The coupling between the superfluid and the normal components is treated in the framework of a semiclassical transport theory for the quasiparticle-distribution function, combined with a hydrodynamic equation for the collective motion of the superfluid component. We develop a numerical test-particle method for solving these equations in the linear response regime. As a first application we study the temperature dependence of the collective quadrupole mode of a Fermi gas in a spherical trap. The coupling between the superfluid collective motion and the quasiparticles leads to a rather strong damping of the hydrodynamic mode already at very low temperatures. At higher temperatures the spectrum has a two-peak structure, the second peak corresponding to the quadrupole mode in the normal phase.

I. INTRODUCTION

Most of the current experiments involving trapped atomic Fermi gases focus on the BEC-BCS crossover. By changing the magnetic field around a Feshbach resonance, the scattering length a of the atoms can be varied from small positive values through very large values near the resonance to small negative values. For $a > 0$, $k_F a \ll 1$ (where k_F denotes the Fermi momentum) the system can be considered as a Bose-Einstein condensate (BEC) of diatomic molecules. The crossover region, $k_F|a| \gtrsim 1$, is not yet very well understood from a theoretical point of view. Finally, on the other side of the resonance, when $a < 0$, $k_F|a| \ll 1$, the system should be in the BCS phase if the temperature is sufficiently low. However, the BCS critical temperature T_c is extremely low, and very soon the magnetic field reaches the point where T_c becomes smaller than the actual temperature T, and the system undergoes the phase transition to the normal (non-superfluid) phase.

One possibility to study the crossover experimentally is to measure the properties of certain collective oscillations. For example, the radial and axial breathing modes of a cigar-shaped trapped Fermi gas have been measured over the whole crossover region [1, 2]. In these experiments one can observe how the frequencies and damping rates of the modes change from what one expects for a BEC to what one expects for a collisionless normal Fermi gas. Assuming that, except in the collisionless normal phase, hydrodynamics is valid, the measured frequencies can give some information on the equation of state in the crossover region.

However, this schematic picture is not completely accurate. Since the system is in a trap, there is no sharp transition from the superfluid to the normal phase. This can be seen as follows: The BCS critical temperature T_c depends on the atom density ρ, and the density depends on the position $\mathbf{r}$. In the center of the trap, the density

$\rho(\mathbf{r})$ and hence the local critical temperature $T_c(\mathbf{r})$ are higher than in the outer part of the trap. As a consequence, for a given temperature, the outer part gets already normal at a magnetic field where the inner part is still superfluid. To be more precise, a system in the BCS phase at finite temperature behaves effectively like a mixture of superfluid and normal components with densities ρ_s and ρ_n, respectively, which become $\rho_s = \rho$, $\rho_n = 0$ in the limit $T = 0$ and $\rho_s = 0$, $\rho_n = \rho$ in the limit $T \geq T_c$. As a consequence, if $0 < T < T_c(\mathbf{r} = 0)$, the superfluid inner part of the trap behaves like a mixture of normal and superfluid components, while only the outer part with $T_c(\mathbf{r}) < T$ is completely normal [3].

If the collision rate was high enough, also the normal component of the gas would behave hydrodynamically. Such a system could be described by Landau's two-fluid hydrodynamics which has been applied to collective modes in trapped superfluid gases at finite temperature [4]. However, although in the recent experiments the transition to the normal phase seemed to occur at a value of $k_F|a| \approx 2$ [1] (i.e., the BCS phase has not really been reached), the system behaved already like a collisionless normal Fermi gas. Hence it seems to be clear that the normal component cannot be treated in terms of hydrodynamics, but a description in terms of a Vlasov equation is required.

We note that there are other approaches to the description of the collective modes at finite temperature. In particular, let us mention the quasiparticle random phase approximation (QRPA) [5, 6], which can be seen as the linearized form of the time-dependent Bogoliubov-de Gennes (BdG) equations. However, for practical reasons this method is limited to systems with spherical symmetry and numbers of particles up to a few times 10^4. Another disadvantage of this method is that it does not allow to include a collision term.

For the case of clean superconductors, a semiclassical transport theory taking the coupling between normal and superconducting components into account has

been developed by Betbeder-Matibet and Nozières [7]. Transport theories of this type have also been used for describing the dynamics of superfluid ^{3}He [8, 9]. In a preceding paper [10], we derived the semiclassical transport equations for the case of trapped atomic Fermi gases and applied them to the quadrupole mode of a gas in a spherical trap. We found that the presence of the normal component leads to a strong damping of the hydrodynamic collective mode. The same mechanism might explain the strong damping observed experimentally near the transition to the collisionless behavior [1]. However, in Ref. [10] we had to replace the gap $\Delta(\mathbf{r})$ by a constant in order to find an analytical solution of the transport equations. Due to this simplification, which cannot really be justified, the damping of the hydrodynamic mode at a given temperature was much weaker than that obtained in QRPA calculations [6].

In the present paper we will work out a numerical method which allows us to treat the realistic $\mathbf{r}$-dependence of the gap. In addition, the method is very versatile and allows to treat much more general cases than can be solved analytically in the constant-gap approximation. The basic idea is to replace the continuous phase-space distribution function of the quasiparticles by a sum of a finite number of delta functions in phase space, called "test particles." In the normal phase, the test-particle method is routinely used for solving the Vlasov equation, e.g. for simulating heavy-ion collisions in nuclear physics [11]. It has also been applied to the simulation of the dynamics of normal trapped atomic Fermi gases with collision term [12] and of Bose-Fermi mixtures [13]. However, to our knowledge, the test-particle method has not yet been used in the context of superfluid systems, and in fact the numerical difficulties are quite different from those encountered in the usual applications.

The article is organized as follows. In Sec. II, we give a brief summary of the transport equations for the BCS phase and their linearization in the case of small deviations from equilibrium. We also give arguments why some terms which appear in the equations can be neglected. In Sec. III we introduce the test-particle method for the case of small oscillations around equilibrium. We describe in detail a number of tricky points we encountered during the implementation of the method, in particular the calculation of the test-particle trajectories, the generation of the test-particle distribution in phase space, and the initialization after a delta-like perturbation. In Sec. IV we present the first results obtained with the help of this method, again for the quadrupole mode in a spherical system. Finally, in Sec. V, we summarize and draw our conclusions.

II. TRANSPORT EQUATIONS FOR THE BCS PHASE

A. Summary of the kinetic equations

In this subsection we will give a brief summary of the kinetic equation approach developed by Betbeder-Matibet and Nozières [7] for the case of clean superconductors and adapted to the case of trapped atomic Fermi gases in Ref. [10]. In this paper we will only give the final equations. For details of the derivations, see Ref. [10] and the footnote [27].

We consider a dilute gas of fermionic atoms of mass m in two equally populated hyperfine states $\uparrow$ and $\downarrow$, trapped by an external potential V_{ext} and interacting via an attractive short-range interaction which leads to a scattering length $a < 0$. The corresponding classical mean-field hamiltonian (minus the chemical potential μ) reads

$$h(\mathbf{r}, \mathbf{p}) = \frac{\mathbf{p}^2}{2m} + V(\mathbf{r}) - \mu \,, \tag{1}$$

where V denotes the sum of the external and the Hartree potential,

$$V(\mathbf{r}) = V_{ext}(\mathbf{r}) + V_{Hartree}(\mathbf{r}) = V_{ext}(\mathbf{r}) + g\rho(\mathbf{r}) \,. \tag{2}$$

In the latter equation, $g = 4\pi\hbar^2 a/m$ denotes the coupling constant and ρ is the density per spin state. The Vlasov equation (without collision term) for the phase-space distribution function $\varrho(\mathbf{r}, \mathbf{p})$ in the normal phase can be written in the compact form

$$\dot{\varrho} = \{h, \varrho\} \,, \tag{3}$$

where $\{\cdot, \cdot\}$ denotes the Poisson bracket. One way to derive this equation is to perform a Wigner-Kirkwood expansion up to order $\hbar$ of the time-dependent Hartree-Fock equation [11, 14].

In the superfluid phase the derivation of an analogous transport equation is much more complicated due to the presence of the complex order parameter (gap) $\Delta(\mathbf{r})$ whose phase describes the collective motion of the Cooper pairs. In addition to the density matrix ϱ, there exists now an anomalous density matrix (pairing tensor) κ. The gap Δ and the anomalous density are related by the gap equation

$$\Delta(\mathbf{r}) = -g \int \frac{d^3p}{(2\pi\hbar)^3} \left(\kappa(\mathbf{r}, \mathbf{p}) - \frac{\Delta(\mathbf{r})}{p^2/m} \right) \,. \tag{4}$$

The time-dependence of ϱ and κ is governed by the time-dependent Hartree-Fock-Bogoliubov or BdG equations. As in the normal phase, the semiclassical transport theory can be derived from these equations by performing a Wigner-Kirkwood expansion up to order $\hbar$. However, it turns out that it is necessary to introduce a gauge transformation with a phase $\phi(\mathbf{r})$ that makes the order parameter Δ real. This corresponds to a transformation into

the local rest frame of the Cooper pairs, which are moving with the collective velocity $\mathbf{v}_{coll}(\mathbf{r}) = -(\hbar/m)\boldsymbol{\nabla}\phi(\mathbf{r})$. The effect of this transformation is to change the gap Δ, the single-particle hamiltonian h, the normal and anomalous density matrices ϱ and κ according to

$$\tilde{\Delta}(\mathbf{r}) = \Delta(\mathbf{r})e^{2i\phi(\mathbf{r})} \equiv |\Delta(\mathbf{r})|\,, \tag{5}$$

$$\tilde{h}(\mathbf{r},\mathbf{p}) = h[\mathbf{r}, \mathbf{p} - \hbar\boldsymbol{\nabla}\phi(\mathbf{r})] - \hbar\dot{\phi}(\mathbf{r})\,, \tag{6}$$

$$\tilde{\varrho}(\mathbf{r},\mathbf{p}) = \varrho[\mathbf{r}, \mathbf{p} - \hbar\boldsymbol{\nabla}\phi(\mathbf{r})]\,, \tag{7}$$

$$\tilde{\kappa}(\mathbf{r},\mathbf{p}) = \kappa(\mathbf{r},\mathbf{p})e^{2i\phi(\mathbf{r})}\,. \tag{8}$$

Roughly speaking, the phase ϕ determines the dynamics of the superfluid component of the system, while the dynamics of the normal component, consisting of thermally excited quasiparticles, has to be described separately. The distribution of these quasiparticles, denoted by $\nu(\mathbf{r},\mathbf{p})$, obeys the following equation of motion:

$$\dot{\nu} = \{E, \nu\}\,. \tag{9}$$

This equation looks formally very similar to the Vlasov equation (3), except that the hamiltonian h is replaced by the quasiparticle energie E, which is defined as

$$E = \sqrt{\tilde{h}_{ev}^2 + \tilde{\Delta}^2} + \tilde{h}_{od}\,. \tag{10}$$

Throughout this article, the indices "ev" and "od" denote the time-even and time-odd parts of a phase-space function, i.e., the parts which are even and odd in $\mathbf{p}$, respectively. The quasiparticle-distribution function ν is related to the normal and anomalous density matrices in the new gauge, $\tilde{\varrho}$ and $\tilde{\kappa}$, by

$$\tilde{\varrho} = \frac{1}{2} - \frac{\tilde{h}_{ev}}{2E_{ev}}(1 - 2\nu_{ev}) + \nu_{od}\,, \tag{11}$$

$$\mathrm{Re}\,\tilde{\kappa} = \frac{\tilde{\Delta}}{2E_{ev}}(1 - 2\nu_{ev})\,. \tag{12}$$

The Vlasov-like equation (9) has to be complemented with an equation of motion for the phase ϕ. It turns out that ϕ has to be determined from the continuity equation

$$\dot{\rho}(\mathbf{r}) + \boldsymbol{\nabla}\cdot\mathbf{j}(\mathbf{r}) = 0\,, \tag{13}$$

where the density ρ and the current $\mathbf{j}$ are given by

$$\rho(\mathbf{r}) = \int \frac{d^3p}{(2\pi\hbar)^3}\tilde{\varrho}(\mathbf{r},\mathbf{p})\,, \tag{14}$$

$$\mathbf{j}(\mathbf{r}) = \int \frac{d^3p}{(2\pi\hbar)^3}\frac{\mathbf{p}}{m}\tilde{\varrho}(\mathbf{r},\mathbf{p}) - \frac{\hbar}{m}\rho(\mathbf{r})\boldsymbol{\nabla}\phi(\mathbf{r})\,. \tag{15}$$

B. Linearization around equilibrium

Let us now assume that the external potential V_{ext} can be written as

$$V_{ext} = V_{0ext} + V_{1ext}\,, \tag{16}$$

where V_{0ext} is time-independent and V_{1ext} is a small perturbation. The equilibrium quantities (corresponding to the potential V_{0ext}) will be marked by an index "0". In particular, since in equilibrium the gap can be chosen to be real, we have

$$\phi_0 = 0\,, \quad \tilde{h}_0 = h_0\,, \quad \tilde{\Delta}_0 = \Delta_0\,. \tag{17}$$

The quasiparticle distribution function in equilibrium is given by

$$\nu_0(\mathbf{r},\mathbf{p}) = f[E_0(\mathbf{r},\mathbf{p})]\,, \tag{18}$$

where $f(E)$ denotes the Fermi function,

$$f(E) = \frac{1}{e^{E/(k_BT)} + 1}\,. \tag{19}$$

Our aim is to calculate the small deviations from equilibrium induced by the perturbation V_{1ext}, which will be marked by an index "1". To that end we linearize the transport equation (9) for the quasiparticle-distribution function,

$$\dot{\nu}_1 - \{E_0, \nu_1\} = f'(E_0)\{E_1, E_0\}\,, \tag{20}$$

where $f'(E_0) = df/dE_0$. The deviation of the quasiparticle energy, E_1, which appears on the r.h.s., depends itself on ν_1 through the deviation of the Hartree field, $g\rho_1$, and the deviation of the gap, $\tilde{\Delta}_1$. Expressing ρ_1 and $\tilde{\Delta}_1$ in terms of ν_1, we can write Eq. (20) as

$$\dot{\nu}_1 - \{E_0, \nu_1\} =$$
$$-\frac{f'(E_0)}{m}\Big(-\mathbf{p}\cdot\boldsymbol{\nabla}\frac{V_{1ext} + g\rho_{1\nu} - \hbar\dot{\phi}_1}{1 + gA}$$
$$+ \frac{\Delta_0}{E_0^2}\mathbf{p}\cdot\boldsymbol{\nabla}\frac{\Delta_0(V_{1ext} + g\rho_{1\nu} - \hbar\dot{\phi}_1)}{1 + gA}$$
$$+ \frac{h_0}{E_0^2}\mathbf{p}\cdot\boldsymbol{\nabla}\frac{\Delta_0\Delta_{1\nu}}{gA} + \frac{\hbar}{m}\frac{h_0}{E_0}(\mathbf{p}\cdot\boldsymbol{\nabla})^2\phi_1$$
$$- \hbar\frac{h_0}{E_0}(\boldsymbol{\nabla}V_0)\cdot\boldsymbol{\nabla}\phi_1 - \hbar\frac{\Delta_0}{E_0}(\boldsymbol{\nabla}\Delta_0)\cdot\boldsymbol{\nabla}\phi_1\Big)\,. \tag{21}$$

where $\rho_{1\nu}$ and $\Delta_{1\nu}$ are the quasiparticle contributions to ρ_1 and $\tilde{\Delta}_1$,

$$\rho_{1\nu}(\mathbf{r}) = \int \frac{d^3p}{(2\pi\hbar)^3}\frac{h_0(\mathbf{r},\mathbf{p})}{E_0(\mathbf{r},\mathbf{p})}\nu_1(\mathbf{r},\mathbf{p})\,, \tag{22}$$

$$\Delta_{1\nu}(\mathbf{r}) = g\int \frac{d^3p}{(2\pi\hbar)^3}\frac{\Delta_0(\mathbf{r})}{E_0(\mathbf{r},\mathbf{p})}\nu_1(\mathbf{r},\mathbf{p})\,, \tag{23}$$

while $A(\mathbf{r})$ is a function which depends only on equilibrium quantities. The explicit expression for the function $A(\mathbf{r})$ reads

$$A(\mathbf{r}) = \frac{mp_F(\mathbf{r})}{2\pi^2\hbar^3}[1 - \varphi(\mathbf{r})]\,, \tag{24}$$

where the local Fermi momentum $p_F(\mathbf{r})$ is defined as usual by $p_F^2(\mathbf{r})/(2m) = \epsilon_F(\mathbf{r}) = \mu - V_0(\mathbf{r})$, and the temperature dependence of $A(\mathbf{r})$ is governed by the function

$$\varphi(\mathbf{r}) = -\int d\xi \frac{\xi^2}{E_\xi^2} f'(E_\xi) \,, \qquad (25)$$

with $E_\xi = \sqrt{\xi^2 + \Delta_0^2(\mathbf{r})}$. In the two limiting cases $T = 0$ and $T \geq T_c(\mathbf{r})$, the function $\varphi(\mathbf{r})$ takes the values 0 and 1, respectively. As a consequence, $A(\mathbf{r}) = 0$ if $T \geq T_c(\mathbf{r})$.

In order to determine the phase ϕ_1, we also linearize the continuity equation (13):

$$\dot\rho_1(\mathbf{r}) + \boldsymbol\nabla \cdot \mathbf{j}_1(\mathbf{r}) = 0 \,. \qquad (26)$$

Again, we express all quantities in terms of equilibrium quantities and the unknown quantities ν_1 and ϕ_1. According to Eq. (15), the current $\mathbf{j}_1$ can be decomposed into quasiparticle and superfluid contributions,

$$\mathbf{j}_1(\mathbf{r}) = \mathbf{j}_{1\nu}(\mathbf{r}) - \frac{\hbar}{m}\rho_0(\mathbf{r})\boldsymbol\nabla\phi_1(\mathbf{r}) = 0 \,, \qquad (27)$$

where the quasiparticle contribution is given by

$$\mathbf{j}_{1\nu}(\mathbf{r}) = \int \frac{d^3p}{(2\pi\hbar)^3} \frac{\mathbf{p}}{m} \nu_1(\mathbf{r}, \mathbf{p}) \qquad (28)$$

(note that only the time-odd part of ν_1 contributes to the integral, and $\nu_{1od} = \tilde\varrho_{1od}$). The time derivative $\dot\nu_1$ which appears when one writes down the explicit expression for $\dot\rho_1$ can be eliminated with the help of Eq. (21). As a result, the l.h.s. of the continuity equation becomes

$$\dot\rho_1 + \boldsymbol\nabla \cdot \mathbf{j}_1 =$$
$$\frac{A}{1+gA}\Big[\hbar\ddot\phi_1 - \dot V_{1ext} - \Big(\frac{2\pi^2\hbar^3}{mp_F} + g\Big)\frac{\hbar}{m}\boldsymbol\nabla \cdot (\rho_0\boldsymbol\nabla\phi_1)$$
$$+ g\boldsymbol\nabla \cdot \mathbf{j}_{1\nu} + \frac{\Delta_0}{A}\boldsymbol\nabla \cdot \int \frac{d^3p}{(2\pi\hbar)^3}\frac{\Delta_0}{E_0^2}\frac{\mathbf{p}}{m}\nu_1\Big]. \quad (29)$$

As noted in Ref. [10], the continuity equation is trivially satisfied in the normal phase ($T \geq T_c$). This becomes evident if its l.h.s. is written in the form (29), since in the normal phase we have $\Delta_0 = 0$ and $A = 0$.

C. Identification of important and unimportant terms

Eq. (21) is still very complicated. In order to simplify the problem, let us look more closely at the different terms in order to see if some of them are less important than others. The basic assumption being that Δ, k_BT_c, and k_BT are much smaller than ϵ_F, the distribution function is sharply peaked near the Fermi surface. Under this condition it is useful to express the distribution function ν in terms of the variables $\mathbf{r}$, ξ, and $\hat{\mathbf{p}}$ instead of $\mathbf{r}$ and $\mathbf{p}$, where

$$\xi = h_0(\mathbf{p},\mathbf{r}) \approx v_F(\mathbf{r})[|\mathbf{p}| - p_F(\mathbf{r})], \quad \hat{\mathbf{p}} = \frac{\mathbf{p}}{|\mathbf{p}|}, \quad (30)$$

and $v_F(\mathbf{r}) = p_F(\mathbf{r})/m$. In terms of these variables, ν is sharply peaked near $\xi = 0$, and the relevant values of ξ are of the same order of magnitude as Δ, k_BT_c, and k_BT.

If ν_1 is written as a function of the new variables, the Poisson bracket on the l.h.s. of Eq. (21) becomes

$$\{E_0, \nu_1\} = \frac{\Delta_0}{E_0}v_F\hat{\mathbf{p}} \cdot (\boldsymbol\nabla\Delta_0)\frac{\partial\nu_1}{\partial\xi} + \frac{\xi}{E_0}\frac{1}{p_F}(\boldsymbol\nabla V_0) \cdot \frac{\partial\nu_1}{\partial\hat{\mathbf{p}}}$$
$$- \frac{\xi}{E_0}v_F\hat{\mathbf{p}} \cdot \boldsymbol\nabla\nu_1 + \frac{\Delta_0}{E_0}\frac{1}{p_F}(\boldsymbol\nabla\Delta_0) \cdot \frac{\partial\nu_1}{\partial\hat{\mathbf{p}}}, \quad (31)$$

with the short-hand notation

$$\frac{\partial\nu_1}{\partial\hat{\mathbf{p}}} = \frac{\partial\nu_1}{\partial\vartheta_p}\frac{\partial\hat{\mathbf{p}}}{\partial\vartheta_p} + \frac{1}{\sin^2\vartheta_p}\frac{\partial\nu_1}{\partial\varphi_p}\frac{\partial\hat{\mathbf{p}}}{\partial\varphi_p} \qquad (32)$$

where ϑ_p and φ_p denote the angles characterizing the unit vector $\hat{\mathbf{p}} = (\sin\vartheta_p\cos\varphi_p, \sin\vartheta_p\sin\varphi_p, \cos\vartheta_p)$.

In addition to the assumption $\Delta \ll \epsilon_F$, our semiclassical theory requires that all quantities vary slowly in space, i.e., on a length scale L which should be larger than the coherence length $\hbar v_F/(\pi\Delta)$ [15]. Then, using $\Delta_0 \sim E_0 \sim \xi \sim \Delta$, $\boldsymbol\nabla \sim 1/L$, $\partial/\partial\xi \sim 1/\Delta$, and $\partial/\partial\hat{\mathbf{p}} \sim 1$, all terms in Eq. (31) can be estimated to be of the order of magnitude $(v_F/L)\nu_1$, except the last one, which is of the order $(v_F/L)(\Delta/\epsilon_F)\nu_1$. Hence, the last term of Eq. (31) is negligible.

Let us now distinguish different kinds of contributions to ν_1, depending on whether they are even or odd functions in ξ and $\hat{\mathbf{p}}$:

ν_{1oe}: the part of ν_1 which is odd in ξ and even in $\hat{\mathbf{p}}$ describes, roughly speaking, a change of the Fermi momentum, i.e., fluctuations of the density, and contributes to $\rho_{1\nu}$,

$$\rho_{1\nu} \approx \frac{mp_F}{2\pi^2\hbar^3}\int \frac{d\Omega_p}{4\pi}\int d\xi\frac{\xi}{E}\nu_{1oe}, \qquad (33)$$

with $d\Omega_p = \sin\vartheta_p d\vartheta_p d\varphi_p$, while its contribution to $\Delta_{1\nu}$ is suppressed by one power of Δ/ϵ_F and can be neglected.

ν_{1eo}: the part of ν_1 which is even in ξ and odd in $\hat{\mathbf{p}}$ describes a shift of the Fermi sphere and therefore contributes to the current $\mathbf{j}_{1\nu}$,

$$\mathbf{j}_{1\nu} \approx \frac{p_F^2}{2\pi^2\hbar^3}\int \frac{d\Omega_p}{4\pi}\hat{\mathbf{p}}\int d\xi\,\nu_{1eo}, \qquad (34)$$

and also to the other integral in the continuity equation (29).

ν_{1ee}: the part of ν_1 which is even in ξ and in $\hat{\mathbf{p}}$ describes, roughly speaking, a local temperature fluctuation and leads to a non-vanishing value of $\tilde\Delta_1$ (via $\Delta_{1\nu}$),

$$\tilde\Delta_1 \approx -\frac{1}{1-\varphi}\int \frac{d\Omega_p}{4\pi}\int d\xi\frac{\Delta_0}{E}\nu_{1ee}, \qquad (35)$$

while its contribution to $\rho_{1\nu}$ is suppressed by one power of Δ/ϵ_F and can be neglected.

ν_{1oo}: the part of ν_1 which is odd in ξ and odd in $\hat{\mathbf{p}}$ gives only a negligible contribution to the current $\mathbf{j}_{1\nu}$ (suppressed by one power of Δ/ϵ_F).

If one neglects the last term in Eq. (31), the Poisson bracket in Eq. (21) leads only to a coupling between ν_{1eo} and ν_{1oe} and between ν_{1oo} and ν_{1ee}. To be more specific, ν_{1ee} and ν_{1oo} do not contribute to the dynamics of ν_{1oe} and ν_{1eo}. Since we are interested in density oscillations and currents, which are determined by ν_{1oe} and ν_{1eo}, we might wonder if we could disregard completely ν_{1ee} and ν_{1oo}. To that end we have to check that also on the r.h.s. of Eq. (21) there is no term which couples the undesired quantities ν_{1ee} and ν_{1oo} to ν_{1oe} or ν_{1eo}. Actually, on the r.h.s. of Eq. (21) there is no term containing ν_{1oo} and only one term containing ν_{1ee}, namely the third one,

$$-\frac{f'(E_0)}{m}\frac{h_0}{E_0^2}\mathbf{p}\cdot\boldsymbol{\nabla}\frac{\Delta_0\Delta_{1\nu}}{gA}\approx v_F f'(E_0)\frac{\xi}{E_0^2}\hat{\mathbf{p}}\cdot\boldsymbol{\nabla}(\Delta_0\tilde{\Delta}_1)\,.\tag{36}$$

This term clearly contributes to $\dot{\nu}_{1oo}$, but at least to leading order in Δ/ϵ_F it does not contribute to $\dot{\nu}_{1eo}$ or $\dot{\nu}_{1oe}$. In the continuity equation (29), ν_{1ee} and ν_{1oo} do not appear, i.e., the undesired quantities ν_{1ee} and ν_{1oo} do not contribute to the dynamics of ϕ_1, either. We are therefore allowed to disregard them.

Now, since we are not interested any more in ν_{1ee} and ν_{1oo}, we can remove all the terms on the r.h.s. of Eq. (21) which contribute only to the dynamics of these uninteresting quantities. As mentioned above, this is the case for the third term, Eq. (36), which contributes only to $\dot{\nu}_{1oo}$. The last term on the r.h.s. of Eq. (21),

$$\frac{f'(E_0)}{m}\hbar\frac{\Delta_0}{E_0}(\boldsymbol{\nabla}\Delta_0)\cdot\boldsymbol{\nabla}\phi_1\tag{37}$$

can be omitted, too, since it contributes only to $\dot{\nu}_{1ee}$. In conclusion, we are left with a simplified version of Eq. (21), which reads

$$\dot{\nu}_1 - \{E_0,\nu_1\} =$$
$$-\frac{f'(E_0)}{m}\Big(-\mathbf{p}\cdot\boldsymbol{\nabla}\frac{V_{1ext}+g\rho_{1\nu}-\hbar\dot{\phi}_1}{1+gA}$$
$$+\frac{\Delta_0}{E_0^2}\mathbf{p}\cdot\boldsymbol{\nabla}\frac{\Delta_0(V_{1ext}+g\rho_{1\nu}-\hbar\dot{\phi}_1)}{1+gA}$$
$$+\frac{\hbar}{m}\frac{h_0}{E_0}(\mathbf{p}\cdot\boldsymbol{\nabla})^2\phi_1 - \hbar\frac{h_0}{E_0}(\boldsymbol{\nabla}V_0)\cdot\boldsymbol{\nabla}\phi_1\Big)\,.\tag{38}$$

III. TEST-PARTICLE METHOD

A. Description of the method

The aim of the present work is to solve the Vlasov-like equation (9) for the quasiparticle-distribution function ν together with the continuity equation (13) for the phase of the order parameter with the help of the test-particle method, in analogy to the test-particle method which is used to solve the usual Boltzmann equation. The basic idea of this method is to replace the continuous distribution function $\nu(\mathbf{r},\mathbf{p})$ by a sum of delta functions in phase space,

$$\nu(\mathbf{r},\mathbf{p};t)\propto\sum_i\delta[\mathbf{r}-\mathbf{R}_i(t)]\delta[\mathbf{p}-\mathbf{P}_i(t)]\,,\tag{39}$$

corresponding to a finite number of test particles, each of which follows the classical equation of motion

$$\dot{\mathbf{R}}_i=\frac{\partial E(\mathbf{R}_i,\mathbf{P}_i;t)}{\partial\mathbf{P}_i}\,,\quad\dot{\mathbf{P}}_i=-\frac{\partial E(\mathbf{R}_i,\mathbf{P}_i;t)}{\partial\mathbf{R}_i}\,,\tag{40}$$

as can be seen by inserting Eq. (39) into Eq. (9). Note that, contrary to the usual test-particle method, our test particles here cannot be identified with real particles but rather with Bogoliubov quasiparticles. In its general form, the test-particle method can be applied to situations far from equilibrium. However, here we are only interested in the linear-response regime, i.e., in the limit of small deviations from equilibrium. In this case it is possible to formulate the method in such a way that only the classical trajectories corresponding to the unperturbed system appear.

To that end, we make the following ansatz for the deviation of the distribution function from equilibrium:

$$\nu_1(\mathbf{r},\mathbf{p};t)=-y(\mathbf{r},\mathbf{p};t)f'[E_0(\mathbf{r},\mathbf{p})]\,.\tag{41}$$

Inserting this into the linearized transport equation (38), we obtain the following equation of motion for the function y:

$$\dot{y}(\mathbf{r},\mathbf{p};t)-\{E_0(\mathbf{r},\mathbf{p}),y(\mathbf{r},\mathbf{p};t)\}=F(\mathbf{r},\mathbf{p};t)\,,\tag{42}$$

where

$$F(\mathbf{r},\mathbf{p};t)=-\frac{\mathbf{p}}{m}\cdot\boldsymbol{\nabla}\frac{V_{1ext}+g\rho_{1\nu}-\hbar\dot{\phi}_1}{1+gA}$$
$$+\frac{\Delta_0}{E_0^2}\frac{\mathbf{p}}{m}\cdot\boldsymbol{\nabla}\frac{\Delta_0(V_{1ext}+g\rho_{1\nu}-\hbar\dot{\phi}_1)}{1+gA}$$
$$+\hbar\frac{h_0}{E_0}\Big(\frac{\mathbf{p}}{m}\cdot\boldsymbol{\nabla}\Big)^2\phi_1-\frac{\hbar}{m}\frac{h_0}{E_0}(\boldsymbol{\nabla}V_0)\cdot\boldsymbol{\nabla}\phi_1\,.\tag{43}$$

Denoting by $\mathbf{R}(\mathbf{r},\mathbf{p};t)$ and $\mathbf{P}(\mathbf{r},\mathbf{p};t)$ the classical trajectories satisfying the equations of motion

$$\dot{\mathbf{R}}=\frac{\partial E_0(\mathbf{R},\mathbf{P})}{\partial\mathbf{P}}\,,\quad\dot{\mathbf{P}}=-\frac{\partial E_0(\mathbf{R},\mathbf{P})}{\partial\mathbf{R}}\tag{44}$$

with the initial conditions

$$\mathbf{R}(\mathbf{r},\mathbf{p};0)=\mathbf{r}\,,\quad\mathbf{P}(\mathbf{r},\mathbf{p};0)=\mathbf{p}\,,\tag{45}$$

one can easily show that

$$\frac{d}{dt}y[\mathbf{R}(\mathbf{r},\mathbf{p};t),\mathbf{P}(\mathbf{r},\mathbf{p};t);t]=F[\mathbf{R}(\mathbf{r},\mathbf{p};t),\mathbf{P}(\mathbf{r},\mathbf{p};t);t]\,.\tag{46}$$

Let us now replace the quasiparticle-distribution function by N_ν delta functions in phase space. Since the order of magnitude of ν_1 is dominated by $-f'(E_0)$, it is clear that these delta functions should be distributed near the Fermi surface. To be more specific, we choose N_ν points $\mathbf{r}_i$, $\mathbf{p}_i$ in phase space which are distributed according to a probability density which is proportional to $-f'(E_0)$, in such a way that for arbitrary but sufficiently smooth phase-space functions $\chi(\mathbf{r}, \mathbf{p})$ the integral of $\chi(\mathbf{r}, \mathbf{p})$ times the function $f'[E_0(\mathbf{r}, \mathbf{p})]$ can be approximated by

$$\int \frac{d^3 r \, d^3 p}{(2\pi\hbar)^3} \chi(\mathbf{r}, \mathbf{p}) f'[E_0(\mathbf{r}, \mathbf{p})] \approx -C \sum_{i=1}^{N_\nu} \chi(\mathbf{r}_i, \mathbf{p}_i). \quad (47)$$

Note that, if $\mathbf{r}_i$, $\mathbf{p}_i$ are distributed in such a way, the same is true for $\mathbf{R}_i(t) = \mathbf{R}(\mathbf{r}_i, \mathbf{p}_i; t)$, $\mathbf{P}_i(t) = \mathbf{P}(\mathbf{r}_i, \mathbf{p}_i; t)$, since the quasiparticle energy $E_i = E_0[\mathbf{R}_i(t), \mathbf{P}_i(t)]$ is a constant of the motion. In particular, defining $y_i(t) = y[\mathbf{R}_i(t), \mathbf{P}_i(t); t]$ and using Eq. (47), we can approximate the integral of an arbitrary function χ times the distribution function ν_1 as

$$\int \frac{d^3 r \, d^3 p}{(2\pi\hbar)^3} \chi(\mathbf{r}, \mathbf{p}) \nu_1(\mathbf{r}, \mathbf{p}; t) \approx C \sum_{i=1}^{N_\nu} y_i(t) \chi[\mathbf{R}_i(t), \mathbf{P}_i(t)]. \quad (48)$$

In other words, we have replaced ν_1 by

$$\nu_1(\mathbf{r}, \mathbf{p}; t) \to C \sum_{i=1}^{N_\nu} y_i(t) \delta[\mathbf{r} - \mathbf{R}_i(t)] \delta[\mathbf{p} - \mathbf{P}_i(t)]. \quad (49)$$

According to Eq. (46), the equation of motion of the coefficients y_i is reduced to

$$\dot{y}_i(t) = F[\mathbf{R}_i(t), \mathbf{P}_i(t); t]. \quad (50)$$

Above we assumed the function $\chi(\mathbf{r}, \mathbf{p})$ to be sufficiently smooth. Of course, this causes some trouble if we want to calculate local quantities like the density or the current. For instance, we obtain

$$\rho_{1\nu}(\mathbf{r}) = C \sum_{i=1}^{N_\nu} y_i(t) \frac{\xi_i(t)}{E_i} \delta[\mathbf{r} - \mathbf{R}_i(t)], \quad (51)$$

where $\xi_i(t) = h_0[\mathbf{R}_i(t), \mathbf{P}_i(t)]$. This result makes sense only after the delta functions have been averaged over a volume containing a sufficiently large number of test particles in order to have a reasonable statistics. Supposing that this can be done, and supposing that $V_{ext}(\mathbf{r}; t)$ and the phase $\phi_1(\mathbf{r}; t)$ are known, we can use the result for $\rho_{1\nu}$ in the explicit expression for F in order to obtain a system of N_ν coupled first-order differential equations of the form (50) for the coefficients y_i. This represents a tremendous simplification with respect to the original partial differential equation (38) in seven dimensions ($\mathbf{r}$, $\mathbf{p}$, and t).

However, the phase $\phi_1(\mathbf{r}, t)$ is not known, but it has to be determined from the continuity equation (26). This is, again, very difficult. Hence, instead of solving the continuity equation exactly, we make an ansatz for ϕ_1 and determine the parameters by minimizing the violation of the continuity equation,

$$\int d^3 r (\dot{\rho}_1 + \mathbf{\nabla} \cdot \mathbf{j}_1)^2 = \min, \quad (52)$$

the explicit expression for $\dot{\rho}_1 + \mathbf{\nabla} \cdot \mathbf{j}_1$ being given by Eq. (29). The idea is to expand ϕ_1 on an appropriately chosen set of orthogonal functions ψ_n,

$$\phi_1(\mathbf{r}; t) = \sum_{n=1}^{N_\phi} x_n(t) \psi_n(\mathbf{r}). \quad (53)$$

Inserting this ansatz into Eq. (29), we see that the integral in Eq. (52) depends on x_n and $\ddot{x}_n$. At a given time, we regard x_n and $\dot{x}_n$ as given (e.g., at the moment when the perturbation is switched on, we know that $x_n = \dot{x}_n = 0$). Hence, in order to have a minimal violation of the continuity equation, we have to minimize Eq. (52) with respect to $\ddot{x}_n$ by demanding

$$\frac{d}{d\ddot{x}_n} \int d^3 r (\dot{\rho}_1 + \mathbf{\nabla} \cdot \mathbf{j}_1)^2 = 0. \quad (54)$$

At this stage it turns out to be convenient to choose the basis functions ψ_n such that they satisfy the orthogonality relation

$$\int d^3 r \left(\frac{\hbar A}{1 + gA}\right)^2 \psi_n(\mathbf{r}) \psi_m(\mathbf{r}) = \delta_{nm}. \quad (55)$$

Then we obtain the following differential equation for the coefficients x_n:

$$\ddot{x}_n(t) = \sum_{m=1}^{N_\phi} a_{nm} x_m(t) + \int d^3 r \frac{\hbar A^2 \psi_n}{(1 + gA)^2} \left(\dot{V}_{1ext} - g\mathbf{\nabla} \cdot \mathbf{j}_{1\nu} - \frac{\Delta_0}{A} \mathbf{\nabla} \cdot \int \frac{d^3 p}{(2\pi\hbar)^3} \frac{\Delta_0}{E_0^2} \frac{\mathbf{p}}{m} \nu_1 \right), \quad (56)$$

where a is a time-independent matrix,

$$a_{nm} = \frac{\hbar^2}{m} \int d^3 r \frac{A^2 \psi_n}{(1 + gA)^2} \left(\frac{2\pi^2 \hbar^3}{m p_F} + g\right) \mathbf{\nabla} \cdot (\rho_0 \mathbf{\nabla} \psi_m). \quad (57)$$

Using Eq. (48) and integrating by parts, we can rewrite Eq. (56) in a more convenient form as

$$\ddot{x}_n(t) = \sum_{m=1}^{N_\phi} a_{nm} x_m(t) + \sum_{i=1}^{N_\nu} b_{ni}(t) y_i(t) + \dot{v}_n(t), \quad (58)$$

where $b(t)$ denotes the matrix

$$b_{ni}(t) = \frac{\hbar C}{m} \mathbf{P}_i(t) \cdot \left(\mathbf{\nabla} \frac{gA^2 \psi_n}{(1 + gA)^2} + \frac{\Delta_0}{E_i^2} \mathbf{\nabla} \frac{A\Delta_0 \psi_n}{(1 + gA)^2}\right)_{\mathbf{R}_i(t)} \quad (59)$$

and the vector v is defined by

$$v_n = \hbar \int d^3 r \frac{A^2 \psi_n V_{1ext}}{(1 + gA)^2} \,. \qquad (60)$$

Mainly for formal purposes, we note that also the equation (50) for the coefficients y_i can be rewritten in matrix notation as

$$\dot{y}_i(t) = \sum_{n=1}^{N_\phi} [c_{in}(t)\dot{x}_n(t) + d_{in}(t)x_n(t)] + f_i(t)$$
$$+ \sum_{j=1}^{N_\nu} g_{ij}(t)y_j(t)\,, \quad (61)$$

where

$$c_{in}(t) = \frac{\hbar}{m} \mathbf{P}_i(t) \cdot \left(\boldsymbol{\nabla} \frac{\psi_n}{1 + gA} - \frac{\Delta_0}{E_i^2} \boldsymbol{\nabla} \frac{\Delta_0 \psi_n}{1 + gA} \right)_{\mathbf{R}_i(t)}, \qquad (62)$$

$$d_{in}(t) = \frac{\hbar}{m} \frac{\xi_i(t)}{E_i} \left(\frac{(\mathbf{P}_i(t) \cdot \boldsymbol{\nabla})^2 \psi_n}{m} - (\boldsymbol{\nabla} V_0) \cdot \boldsymbol{\nabla} \psi_n \right)_{\mathbf{R}_i(t)}, \qquad (63)$$

$$f_i(t) = -\frac{\mathbf{P}_i(t)}{m} \cdot \left(\boldsymbol{\nabla} \frac{V_{1ext}}{1 + gA} - \frac{\Delta_0}{E_i^2} \boldsymbol{\nabla} \frac{\Delta_0 V_{1ext}}{1 + gA} \right)_{\mathbf{R}_i(t)}, \qquad (64)$$

and

$$g_{ij}(t) = -gC \frac{\xi_j(t)}{E_j} \frac{\mathbf{P}_i(t)}{m} \cdot \left(\boldsymbol{\nabla} \frac{\tilde{\delta}[\mathbf{r} - \mathbf{R}_j(t)]}{1 + gA} \right.$$
$$\left. - \frac{\Delta_0}{E_i^2} \boldsymbol{\nabla} \frac{\Delta_0 \tilde{\delta}[\mathbf{r} - \mathbf{R}_j(t)]}{1 + gA} \right)_{\mathbf{R}_i(t)}. \qquad (65)$$

In the latter equation, $\tilde{\delta}$ denotes a kind of "smeared" delta function which accounts for the averaging mentioned below Eq. (51).

However, as mentioned above, Eqs. (61) and (65) will be used for formal purposes only. In practice, it is much faster to calculate $\rho_{1\nu}(\mathbf{r})$ after each time step on a discrete mesh, and to interpolate the stored values when performing the next time step for the coefficients y_i. For the calculation of $\rho_{1\nu}(\mathbf{r})$, we replace the delta function in Eq. (51) by a Gaussian having a width d_ρ.

In summary, the coupled system of partial differential equations, namely the transport equation for the distribution function ν_1 and the continuity equation for the phase ϕ_1 [Eqs. (38) and (26)], has been replaced by a coupled system of ordinary linear differential equations for the coefficients y_i and x_n [Eqs. (61) and (58)], which can formally be written as

$$\frac{d}{dt} \begin{pmatrix} x(t) \\ \dot{x}(t) \\ y(t) \end{pmatrix} = \begin{pmatrix} 0 & 1 & 0 \\ a & 0 & b(t) \\ d(t) & c(t) & g(t) \end{pmatrix} \begin{pmatrix} x(t) \\ \dot{x}(t) \\ y(t) \end{pmatrix} + \begin{pmatrix} 0 \\ \dot{v}(t) \\ f(t) \end{pmatrix}. \qquad (66)$$

B. Trajectories of the test particles

In practice, the solution of the classical equations of motion for the test particles, Eqs. (44), faces us with some unusual features which are not present with the usual Newtonian equations of motion. Note that we are not dealing with ordinary particles but with Bogoliubov quasiparticles, which have some surprising properties. For instance, E_i being a constant of the motion and $E_i^2 = \xi_i^2 + \Delta_0^2(\mathbf{r}_i)$, it is evident that the energy ξ_i cannot be conserved if the gap Δ_0 depends on $\mathbf{r}$. In particular, when a test particle with quasiparticle energy E_i reaches the surface where $\Delta_0(\mathbf{r}) = E_i$, it is reflected (Andreev reflection). During this reflection, the momentum $\mathbf{P}_i$ stays almost constant, but the energy ξ_i changes its sign (i.e., a particle is transformed into a hole or vice versa), such that the velocity $\mathbf{v}_i = \partial E_i/\partial \mathbf{P}_i = (\xi_i/E_i)\mathbf{P}_i/m$ is reversed. As a consequence, the quasiparticle is reflected into the direction where it came from, which is very surprising if the incident angle is different from $90°$.

In order to find the test-particle trajectories numerically, it does not seem very efficient to start directly from Eqs. (44), since a small numerical error in the momentum of the order of $\delta P/P \sim \Delta/\epsilon_F$ would immediately lead to a completely wrong behavior. It is therefore advantageous to make use of the variable ξ_i, whose equation of motion reads

$$\dot{\xi}_i = -\frac{\Delta_0(\mathbf{R}_i)}{E_i} \frac{\mathbf{P}_i}{m} \cdot \boldsymbol{\nabla}\Delta_0(\mathbf{R}_i)\,. \qquad (67)$$

Solving this equation together with the equations for $\mathbf{R}_i$ and $\mathbf{P}_i$, we can correct $\mathbf{P}_i$ after each time step according to

$$\mathbf{P}_i^{corr.} = \frac{\mathbf{P}_i}{|\mathbf{P}_i|} \sqrt{2m\xi_i + p_F^2(\mathbf{R}_i)}\,. \qquad (68)$$

In practice, the variable ξ_i also allows us to introduce a very reliable method for determining the step size. Let us denote by ξ_i' the result we obtain after one time step of size δt, and by ξ_i'' the result we obtain after two time steps of size $\delta t/2$ each. Then the quantity $\delta t|\xi' - \xi''|$ is a measure for the numerical error and can be used for adapting the step size δt to the situation. It turns out that the step size has to become very small only during Andreev reflection.

Now let us give some examples for typical test-particle trajectories. For that purpose, let us restrict ourselves to the most simple case which is a spherical harmonic trap,

$$V_{0ext}(\mathbf{r}) = \frac{1}{2} m\Omega^2 r^2\,. \qquad (69)$$

This potential defines the so-called trap units, i.e., energies are measured in units of $\hbar\Omega$, temperatures in units of $\hbar\Omega/k_B$, lengths in units of $l_{ho} = \sqrt{\hbar/(m\Omega)}$, etc. In this example, due to spherical symmetry, not only the quasiparticle energy E, but also the angular momentum $\mathbf{L} = \mathbf{r} \times \mathbf{p}$ of a test particle is a constant of the motion.

Within the local-density approximation (LDA) [16, 17], the density $\rho_0(r)$ has its maximum at the center of the trap and vanishes approximately (except for very small temperature effects) at the Thomas-Fermi radius $R_{TF} = \sqrt{2\mu/(m\Omega^2)}$. The gap $\Delta_0(r)$ has its maximum at the center of the trap, too, and goes to zero at some critical radius R_c which is temperature dependent and determined by the equation $T = T_c(R_c)$. In order to avoid numerical problems arising from the infinite derivative of $\Delta_0(r)$ at $r = R_c$, we convolute the LDA result for $\Delta_0(r)$ with a Gaussian of width d_Δ. In fact, this is more realistic than the LDA result since the exact solution of the BdG equations also leads to a gap $\Delta_0(r)$ which has an exponential tail [17, 18, 19]. As parameters we choose $\mu = 32\,\hbar\Omega$, $g = -\hbar^2 l_{ho}/m$, and $T = 1.4\,\hbar\Omega/k_B$. The corresponding number of atoms in the trap is approximately 1.7×10^4. For these parameters quantum mechanical (BdG, QRPA) results are available for comparison. The width d_Δ is chosen such as to optimize the agreement with the BdG gap, which for the present parameters is achieved with $d_\Delta = l_{ho}$.

In Fig. 1 we show the corresponding gap $\Delta_0(r)$ as a function of the distance r from the center of the trap. From this figure it is evident that due to the condition $E \geq \Delta_0(r)$, the relevant quasiparticles (having $E \lesssim k_B T = 1.4\,\hbar\Omega$) are excluded from the region $r \lesssim 4l_{ho}$. In addition to the gap, we display the potential $V_0(r) - \mu$, since the motion of a quasiparticle with given energy E and angular momentum $\mathbf{L}$ is also limited by the condition $\sqrt{E^2 - \Delta_0^2(r)} - \mathbf{L}^2/2mr^2 \geq V_0(r) - \mu$. It has been shown that also within the fully quantum-mechanical BdG theory the lowest-lying quasiparticle states are localized in this region [20]. In our example, the motion of the relevant quasiparticles is restricted to the region $4 \lesssim r/l_{ho} \lesssim 8$.

Most of these quasiparticles will undergo Andreev reflection. Their trajectories are approximately described by an ellipse which is cut at the points where $\Delta_0(r) = E$. If $E \ll \epsilon_F$, the quasiparticle will move hence and forth on the same partial ellipse. Such trajectories with $E = 0.1\,\hbar\Omega$ and $0.4\,\hbar\Omega$ are shown in the left panel of Fig. 2. However, if the quasiparticle energy is higher, the change in energy from $\xi \approx E$ to $\xi \approx -E$ (or vice versa) during the Andreev reflection results in a change of momentum which is no more negligible. Then, due to angular momentum conservation, the angle of reflection is slightly different from the angle of incidence, and the whole trajectory is precessing. An example for such a trajectory with $E = 0.7\,\hbar\Omega$ is also shown in the left panel of Fig. 2. A completely different picture arises if the initial conditions are such that the quasiparticle does never reach the point where $\Delta(r) = E$. Then the trajectory is just a precessing, slightly deformed ellipse, as shown in the right panel of Fig. 2 for the case of a trajectory with $E = \hbar\Omega$. There is a striking analogy between these trajectories and the "glancing" orbits discussed, e.g., in Ref. [21] in the context of a superconducting cylinder which is coated by a normal-metal layer.
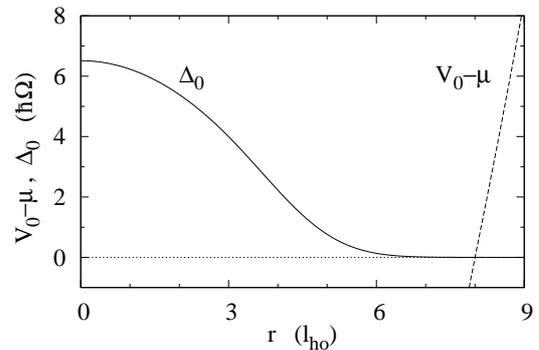

FIG. 1: Gap $\Delta_0(r)$ (solid line) and potential $V_0(r) - \mu$ (dashed line) for the case of a spherical trap with frequency Ω, chemical potential $\mu = 32\,\hbar\Omega$, coupling constant $g = -\hbar^2 l_{ho}/m$, and temperature $k_B T = 1.4\,\hbar\Omega$. Δ_0 and $V_0 - \mu$ are in units of $\hbar\Omega$, r is in units of the oscillator length l_{ho}. Roughly speaking, these two curves determine the classically allowed region for a quasiparticle with given energy E.
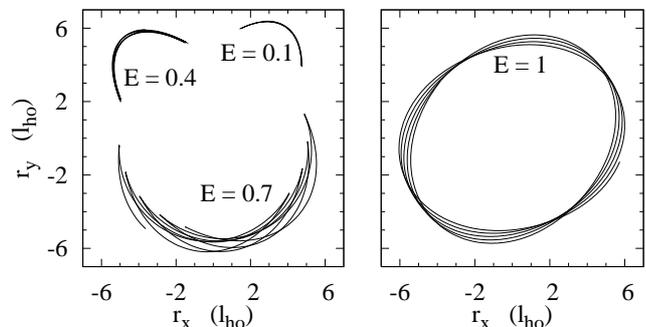

FIG. 2: Four examples of quasiparticle trajectories in a trap with parameters given below Fig. 1. The three trajectories shown in the left panel belong to quasiparticles with $E = 0.1\,\hbar\Omega$, $0.4\,\hbar\Omega$, and $0.7\,\hbar\Omega$, respectively. The trajectory displayed in the right panel belongs to a quasiparticle with $E = \hbar\Omega$.

C. Distribution of test particles in phase space

In Sec. III A we supposed that one can generate a distribution of points $\mathbf{r}_i$, $\mathbf{p}_i$ in phase space such that Eq. (47) is approximately satisfied for sufficiently smooth functions $\chi(\mathbf{r}, \mathbf{p})$. In practice, this distribution is obtained in two steps. First we generate the coordinates $\mathbf{r}_i$, and in a second step the momenta $\mathbf{p}_i$.

The mean density of test particles at a certain point $\mathbf{r}$ is given by

$$n(\mathbf{r}) = \sum_{i=1}^{N_\nu} \tilde{\delta}(\mathbf{r}_i - \mathbf{r})\,, \qquad (70)$$

where $\tilde{\delta}$ denotes a smeared delta function in order to

account for the averaging. Using Eq. (47), we conclude

$$n(\mathbf{r}) = -\frac{1}{C} \int \frac{d^3p}{(2\pi\hbar)^3} f'[E_0(\mathbf{r}, \mathbf{p})] \equiv \frac{w(\mathbf{r})}{C}. \qquad (71)$$

The algorithm for the generation of the coordinates $\mathbf{r}_i$ is now very simple. First we look for the maximum w_{max} of the function $w(\mathbf{r})$. Defining $P(\mathbf{r}) = w(\mathbf{r})/w_{max}$, we obtain a function whose values lie between 0 and 1. Then we generate uniformly distributed random points $\mathbf{r}_k$ in a volume which contains the whole system, and retain each point with the probability $P(\mathbf{r}_k)$, until the desired number of points, N_ν, is reached.

The formula (71) for the test-particle density $n(\mathbf{r})$ can also be used for the determination of the normalization constant C. Integrating $n(\mathbf{r})$ over space, we must recover the total number of test particles. This implies

$$C = \frac{1}{N_\nu} \int d^3r \, w(\mathbf{r}). \qquad (72)$$

Now we turn to the distribution of the momenta $\mathbf{p}_i$. It is evident that the angular distribution of the momenta is isotropic, i.e., the interesting part of the problem is the distribution of the absolute values, $p_i = |\mathbf{p}_i|$, which is, of course, directly related to the distribution of the energies ξ_i. Let us define the mean number of test particles per energy and volume

$$n(\mathbf{r}, \xi) = \sum_{i=1}^{N_\nu} \tilde{\delta}(\mathbf{r}_i - \mathbf{r})\tilde{\delta}(\xi_i - \xi). \qquad (73)$$

Again, with the help of Eq. (47), this becomes

$$n(\mathbf{r}, \xi) = -\frac{1}{C} \frac{m p_\xi}{2\pi^2\hbar^3} f'(E_\xi), \qquad (74)$$

with $p_\xi = \sqrt{2m\xi + p_F^2(\mathbf{r})}$, i.e., for given spatial coordinates $\mathbf{r}$, the probability density for finding a particle at energy ξ is proportional to $-p_\xi f'(E_\xi)$. Such a distribution can be generated in the following way. Starting from random numbers z_k which are uniformly distributed in the interval $(0, 1)$, it is straight-forward to show that the energies

$$\xi_k = T \ln \frac{z_k}{1 - z_k} \qquad (75)$$

are distributed according to the probability density $-f'(\xi)$. It is evident that negative energies with $\xi < -\epsilon_F(\mathbf{r})$ have to be removed. Furthermore, it is preferable to cut the distribution at energies which lie too far away from the Fermi surface, e.g., $|\xi| > 15T$ (the probability that this happens is less than 10^{-6}). The momenta p_ξ are thus limited by $p_{max} = \sqrt{30mT + p_F^2(\mathbf{r})}$, and the function defined by $P(\xi) = p_\xi f'(E_\xi)/p_{max}f'(\xi)$ cannot become greater than 1 and can serve as a probability. If we retain each energy ξ_k generated according to Eq. (75) with the probability $P(\xi_k)$, the remaining energies are distributed according to the desired distribution.
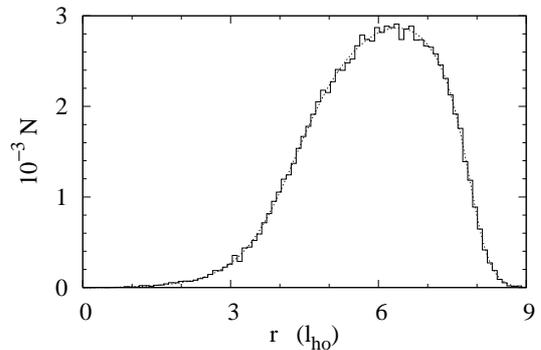

FIG. 3: Radial distribution of 10^5 test particles in a trap with parameters given below Fig. 1, counted in bins of size $\delta r = 0.1 \, l_{ho}$. For comparison, the dotted curve represents the ideal distribution according to Eq. (71).

In order to give an illustration for the resulting distribution of test particles, we show in Fig. 3 the radial distribution of $N_\nu = 10^5$ test particles in a trap with the same parameters as in Fig. 1. In agreement with what we discussed in the preceding subsection, we see that the test particles are mainly located in the region $4 \lesssim r/l_{ho} \lesssim 8$, corresponding to the region where the system is mainly normal fluid. Due to the angular average the statistical fluctuations around the ideal distribution, Eq. (71), which is represented by the dotted line, are very small. We verified that, apart from the statistical fluctuations, our test-particle distribution stays constant, which is a good numerical test of both the initial test-particle distribution and of the test-particle trajectories.

D. Initial condition

In the linear response regime, as the name implies, the response to a time-dependent perturbation of the form $V_1(\mathbf{r}; t) = \hat{V}_1(\mathbf{r})f(t)$, with an arbitrary time dependence $f(t)$, can be obtained as convolution of $f(t)$ with the response to a delta function in time. It is therefore sufficient to study perturbations of the form

$$V_{1\,ext}(\mathbf{r}; t) = \hat{V}_1(\mathbf{r})\delta(t). \qquad (76)$$

We thus set the inhomogeneous terms in Eq. (66) to $\dot{v}(t) = \hat{v}\dot{\delta}(t)$ and $\dot{f}(t) = \hat{f}\delta(t)$, respectively, $\hat{v}$ and $\hat{f}$ being defined analogously to Eqs. (60) and (64) but with $V_{1\,ext}$ replaced by $\hat{V}_1$.

Assuming that the system was in equilibrium before this perturbation, we may ask the question: What are the values of the coefficients y_i and x_n immediately after the perturbation, i.e., at infinitesimally small $t > 0$? This question can be answered exactly, since during the infinitesimal period where the perturbation is active, the matrix in Eq. (66) can be regarded as time-independent. Integrating Eq. (66) over time from $-t_0$ to t_0, we obtain

in the limit $t_0 \to 0$

$$\lim_{t_0 \to 0} \begin{pmatrix} x(t_0) \\ \dot{x}(t_0) \\ y(t_0) \end{pmatrix} = \begin{pmatrix} \hat{v} \\ 0 \\ c\hat{v} + \hat{f} \end{pmatrix}. \qquad (77)$$

Let us now assume that the function $\hat{V}_1$ lies in the space spanned by the functions ψ_n. Then it is evident that the corresponding linear combination is given by the coefficients $\hat{v}_n$, i.e.,

$$\hat{V}_1(\mathbf{r}) = \hbar \sum_{n=1}^{N_\phi} \hat{v}_n \psi_n(\mathbf{r}). \qquad (78)$$

Note that the functions ψ_n do not necessarily have to have this property. For example, we could define a basis of functions satisfying the orthogonality relation (55) and maybe even a suitably defined completeness relation if $N_\phi \to \infty$, but which all vanish identically outside the superfluid region, i.e., in the region where $\Delta_0 = 0$ (and $A = 0$). Eq. (78) would then be satisfied inside the superfluid region, but not outside. Hence, it is an additional requirement for the choice of the functions ψ_n. Combining Eqs. (77) and (78), we find

$$\lim_{t_0 \to 0} \phi_1(\mathbf{r}; t_0) = \frac{1}{\hbar} \hat{V}_1(\mathbf{r}). \qquad (79)$$

Eq. (78) also leads to a simplification of the initial value of the coefficients y_i and the quasiparticle-distribution function. Using the explicit expressions for the matrix $\hat{c}$ and the vector $\hat{f}$ [Eqs. (62) and (64) with V_{1ext} replaced by $\hat{V}_1$], we obtain from the third line of Eq. (77)

$$\lim_{t_0 \to 0} y_i(t_0) = \sum_{n=1}^{N_\phi} c_{in} \hat{v}_n + \hat{f}_i$$
$$= \frac{\mathbf{p}_i}{m} \cdot \left(\boldsymbol{\nabla} \frac{\hbar \sum_{n=1}^{N_\phi} \hat{v}_n \psi_n - \hat{V}_1}{1 + gA} \right.$$
$$\left. - \frac{\Delta_0}{E_i^2} \boldsymbol{\nabla} \frac{\Delta_0(\hbar \sum_{n=1}^{N_\phi} \hat{v}_n \psi_n - \hat{V}_1)}{1 + gA} \right)_{\mathbf{r}_i}. \quad (80)$$

As a consequence, if Eq. (78) is satisfied, the initial values of the coefficients y_i vanish, which implies

$$\lim_{t_0 \to 0} \nu_1(\mathbf{r}, \mathbf{p}; t_0) = 0. \qquad (81)$$

In fact, the simple result of this subsection, which is summarized in Eqs. (79) and (81), could have been anticipated without any calculation. The effect of a perturbation of the form (76) is to give a particle at position $\mathbf{r}$ a kick

$$\delta \mathbf{p} = -\int dt \boldsymbol{\nabla} V_{1ext}(\mathbf{r}; t) = -\boldsymbol{\nabla} \hat{V}_1(\mathbf{r}). \qquad (82)$$

Since this kick does not depend on the momentum of the particle, the local Fermi sphere is shifted as a whole, there

is no change in density and no Fermi surface deformation. Within the present theoretical framework, Cooper pairs are not broken either, they just acquire a center of mass momentum. Thus, the distribution function in the local rest frame stays unchanged ($\nu_1 = 0$), and the collective velocity is given by $\mathbf{v}_{coll} = -(\hbar/m)\boldsymbol{\nabla}\phi_1 = -(1/m)\boldsymbol{\nabla}\hat{V}_1$.

Note, however, that in reality a perturbation which has the form of a short pulse would lead to much more complicated effects (e.g., pair breaking). Since our semiclassical description requires that the time dependence of the perturbation is slow, our formal result for a delta-like excitation becomes physically meaningful only after it has been convoluted with a function $f(t)$ which varies slowly in time. In other words, we can only calculate the low-frequency part of the response function.

IV. FIRST RESULTS

In this section we will discuss first numerical results which have been obtained using the test-particle method. Our intention here is to see whether this method is in principle capable to describe the most important features of collective excitations in superfluid trapped Fermi gases. To that end, we will study the quadrupole excitation of a spherical system, which is excited by

$$\hat{V}_1(\mathbf{r}) = \alpha \, m\Omega(2r_z^2 - r_x^2 - r_y^2) \qquad (83)$$

(the factor $m\Omega$ has been introduced in order to make the coefficient α dimensionless).

For practical purposes, we will make an additional approximation: We will restrict our ansatz for the phase, Eq. (53), to only one or two functions ψ_n. It is clear from rotational symmetry that in the case of a quadrupole excitation of the form (83) the most general form the phase can have is

$$\phi_1(\mathbf{r}) = \Phi(r)[2r_z^2 - r_x^2 - r_y^2], \qquad (84)$$

such that that the functions ψ_n can be written as

$$\psi_n(\mathbf{r}) = \Psi_n(r)[2r_z^2 - r_x^2 - r_y^2]. \qquad (85)$$

It is known from superfluid hydrodynamics that at zero temperature the velocity field is essentially linear in the coordinates, i.e., the function $\Phi(r)$ is almost constant. As a first guess we will assume that this is still true at non-zero temperature, and hence we will take only one single function ($N_\phi = 1$) in the ansatz (53) for the phase, $\Psi_1 = const$. The proportionality constant will be determined from the normalization condition (55).

Such a restricted ansatz means of course that the continuity equation will not be exactly satisfied in the superfluid region (remember that outside the superfluid region the phase has no effect whatsoever). We will therefore improve this initial ansatz by including a second function ($N_\phi = 2$) which allows to modulate $\Phi(r)$ in the superfluid region.

The first idea one might have is to use for $\Psi_n(r)$ polynomials in r^2 and to orthogonalize the resulting functions ψ_n. However, it turns out that this leads to numerical instabilities due to the fast growing of the resulting polynomials outside the superfluid region. Let us explain this effect in some more detail. As seen from the transport equation for the quasiparticle-distribution function, the phase ϕ_1 outside the superfluid region enters directly the dynamics of ν_1. Although the net effect of the phase and of the quasiparticle motion should be independent of the choice of ϕ_1 outside the superfluid region, each of these contributions depends on this choice. If ϕ_1 changes too rapidly, the numerical solution of the equation of motion for the coefficients y_i becomes less accurate and the cancellation of the two effects does not work any more.

We therefore have to look for functions Ψ_n which are linearly independent inside the superfluid region, but which do not grow outside. Here we will choose the functions $\tilde{\Psi}_1(r) = 1$ and $\tilde{\Psi}_2(r) = [1 - \varphi(r)]^2$, where $\varphi(r)$ is the function defined in Eq. (25). The function $\tilde{\Psi}_2(r)$ has its maximum in the center of the trap and goes smoothly to zero at the boundary of the superfluid region. From $\tilde{\Psi}_1$ and $\tilde{\Psi}_2$ the functions Ψ_1 and Ψ_2 are determined according to the orthogonality condition (55) with the help of the Gram-Schmidt orthogonalization method. As we will see, the results obtained with $N_\phi = 1$ and $N_\phi = 2$ are very similar and we therefore claim that they would not change a lot if we included additional functions.

Let us now present the results. As in the examples shown in the preceding section, we consider a spherical harmonic trap with $\mu = 32\hbar\Omega$, containing approximately 1.7×10^4 atoms. The resulting density profile $\rho_0(r)$ is shown in Fig. 4 as the dashed line. The critical temperature within LDA is $T_c = T_c(r = 0) \approx 3.9\,\hbar\Omega/k_B$. As before, the LDA result for the gap $\Delta_0(r)$ is convoluted with a Gaussian having a width $d_\Delta = l_{ho}$. We will study the quadrupole mode for three different temperatures, $T/T_c = 0.2$, 0.4, and 0.6. The equilibrium gap $\Delta_0(r)$ for these three temperatures is also displayed in Fig. 4.

After the system is excited, its shape will oscillate. A measure for this quadrupole deformation is the ratio

$$\frac{\langle 2r_z^2 - r_x^2 - r_y^2 \rangle}{\langle r^2 \rangle_0} \,, \tag{86}$$

where $\langle r^2 \rangle_0$ denotes the mean square radius in equilibrium, which in the present case has the value $\langle r^2 \rangle_0 \approx 23\, l_{ho}^2$. In the linear response, the quadrupole deformation is of course proportional to the strength of the perturbation, and we therefore divide our results by this strength [denoted α in Eq. (83)]. In our simulation we use $N_\nu = 10^5$ test particles, the width of the Gaussians used for smearing $\rho_{1\nu}$ (see Sec. III A) is set to $d_\rho = l_{ho}$. In Fig. 5 we display the time dependence of the quadrupole deformation after the perturbation for the three temperatures mentioned before. The corresponding spectra, obtained by Fourier transformation, are shown in Fig. 6. The results for the two cases $N_\phi = 1$ and $N_\phi = 2$ are displayed as dashed and solid curves, respectively. In all
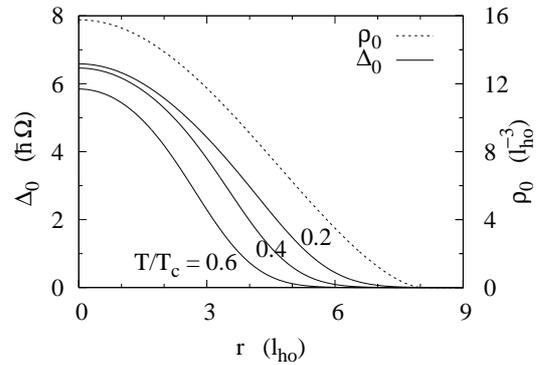

FIG. 4: Density profile $\rho_0(r)$ (dashed line) and gap $\Delta_0(r)$ (solid lines) in a spherical harmonic trap containing 1.7×10^4 atoms ($\mu = 32\,\hbar\Omega$, interaction strength $g = -\hbar^2 l_{ho}/m$). The gap is displayed for three different temperatures, $T/T_c = 0.2$, 0.4, and 0.6, while the density profile is practically independent of T.

cases the two curves are in reasonable agreement, such that we can say that the use of $N_\phi = 2$ independent functions in the ansatz for the phase is sufficient.

We see that the temperature dependence of the spectrum is highly non-trivial. At low temperatures (upper panel of Fig. 6), we see essentially the hydrodynamic quadrupole mode, which at zero temperature lies at $\omega = \sqrt{2}\Omega$ [22, 23, 24] and which is now damped as a consequence of its coupling to the normal component. At higher temperatures (middle of Fig. 6), a second peak builds up in the spectrum, corresponding to the quadrupole mode in the normal phase, which lies slightly above $\omega = 2\Omega$ [25] (for the present set of parameters, its frequency is $\omega \approx 2.2\,\Omega$ [6]). As the temperature approaches T_c (lower panel of Fig. 6), the strength contained in this second peak increases, while the hydrodynamic mode, whose frequency is slightly shifted downwards, disappears. These findings are in good agreement with quantum mechanical QRPA calculations [6].

We note that the damping width of the hydrodynamic mode at low temperature is now comparable with that found within the QRPA and much stronger than that found in our previous work [10], where we replaced the gap $\Delta_0(r)$ by a constant. The reason is in fact very simple: With a constant gap, the fraction ρ_n/ρ_0 of the normal component is independent of r, whereas in the case of an r-dependent gap the normal component in the outer part of the system is already important at very low temperatures [3].

As the temperature T approaches T_c, the quadrupole mode of the normal phase (that at $\omega = 2.2\,\Omega$) becomes undamped, as it is the case within the QRPA. However, even though collisions are strongly suppressed at these low temperatures, it should be kept in mind that the collision term, which is neglected in the present work, is non-zero and its inclusion would lead to a finite lifetime of this oscillation, too.

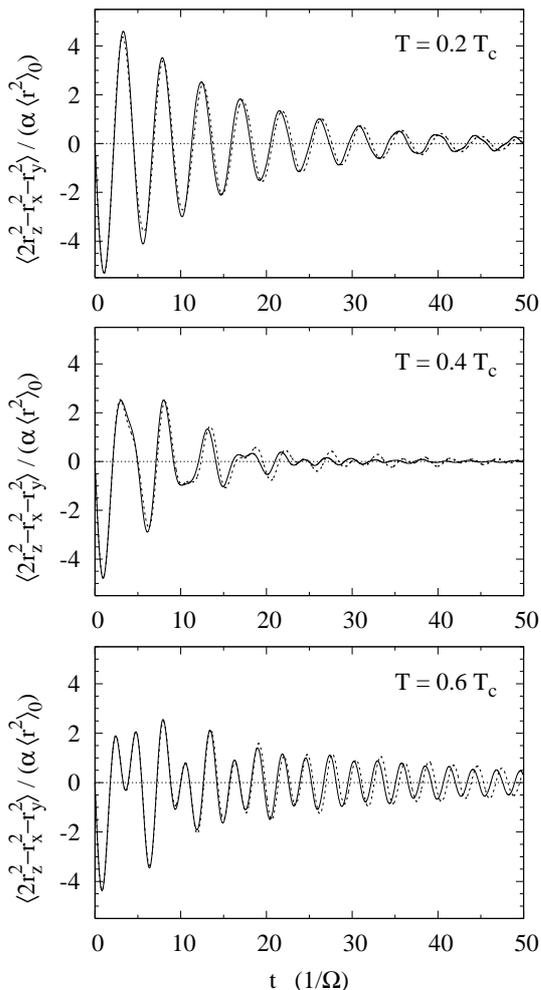Finally, let us compare our semiclassical results more

FIG. 5: Time dependence of the quadrupole deformation after a delta-like perturbation at $t = 0$. The parameters are the same as in Fig. 4, the three panels correspond, from top to bottom, to $T/T_c = 0.2$, 0.4, and 0.6. The dashed and solid lines correspond to $N_\phi = 1$ and $N_\phi = 2$, respectively.
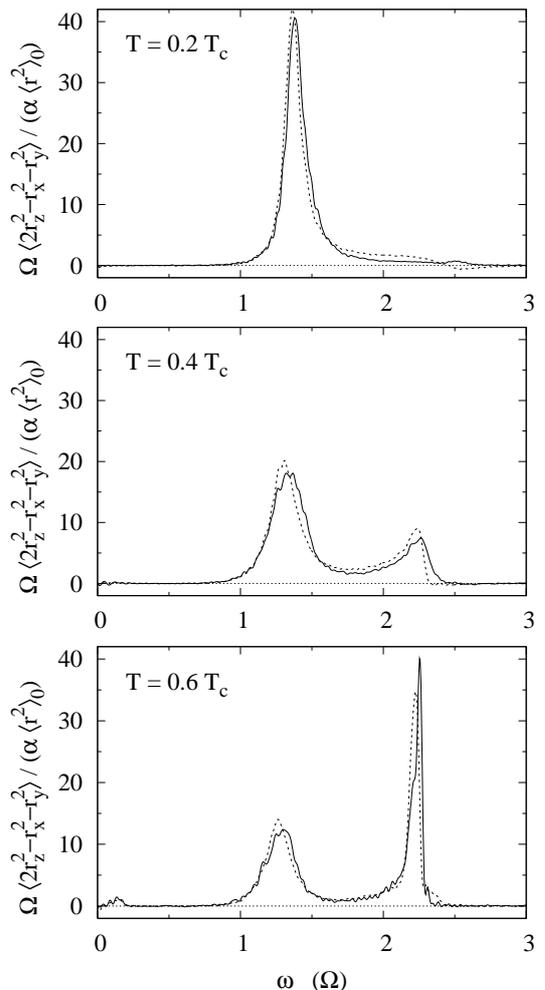

FIG. 6: Fourier transforms of the quadrupole responses shown in Fig. 5.
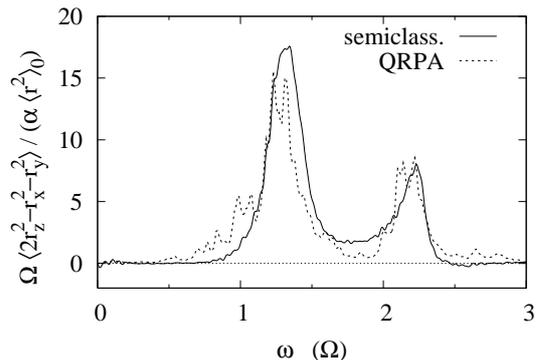

FIG. 7: Quantitative comparison between the semiclassical and the QRPA result for the quadrupole excitation spectrum of a system with $\mu = 32\hbar\Omega$, $g = -0.965\,\hbar^2 l_{ho}/m$, $k_B T = 1.4\,\hbar\Omega$. The semiclassical result (solid line) was obtained with $N_\phi = 2$ basis functions for the phase. The QRPA result (dotted line) was taken from Ref. [6].

quantitatively to quantum mechanical QRPA results. In Fig. 7 we show the QRPA result of Ref. [6] for the quadrupole excitation spectrum (dotted line) together with the semiclassical result we obtain with the same parameters (solid line). As one can see, the total normalization and the relative weights of the two peaks are in reasonable agreement. Also the widths of the QRPA peaks are well reproduced by the semiclassical calculation. The main differences are that within the semiclassical calculation the two peaks lie a bit too high and that they are not as well separated as within the QRPA. A comparison of the two curves for $N_\phi = 1$ and $N_\phi = 2$ in the $T/T_c = 0.4$ case shown in the middle of Fig. 6, whose parameters are quite close to those of Fig. 7, suggests that the latter effect might be partly due to the restricted ansatz for the phase. However, as one can deduce from the irregular structure of the QRPA spectrum, even in a system with 32000 atoms shell effects, i.e., effects which

depend on the discrete single-particle spectrum, are still quite pronounced. It is clear that such effects cannot be reproduced within a semiclassical calculation. In this sense the agreement between the two spectra is very satisfactory, in particular since one can assume that the shell effects decrease with increasing number of particles.

V. CONCLUSIONS

In this paper, we developed a numerical test-particle method for solving the semiclassical transport equations for an ultracold trapped Fermi gas in the BCS phase in the collisionless limit. These transport equations take into account the coupling between the dynamics of the Cooper pairs (superfluid component) and the thermally excited Bogoliubov quasiparticles (normal component). We developed the method for the case of small deviations from equilibrium, so that the test-particle trajectories can be calculated in the equilibrium state. Since the test-particles describe Bogoliubov quasiparticles rather than real particles, the trajectories have very unusual properties compared with the trajectories one has to deal with when applying the test-particle method to the normal Vlasov equation. Our test particles can have the character of particles as well as holes, depending on whether their energy ξ is positive or negative, and they can also be transformed from the one into the other if they hit the region where the gap Δ becomes larger than their quasiparticle energy E (Andreev reflection). Another complication as compared with the normal Vlasov equation is that the dynamics of the quasiparticles is coupled to the collective motion of the superfluid component, which is described by the phase ϕ of the order parameter. This phase has to be determined simultaneously with the evolution of the quasiparticle-distribution function by solving the continuity equation. In the present work, we make an ansatz for ϕ with time-dependent coefficients, leading to an approximate solution of the continuity equation.

As a first application, we calculated the response of a gas trapped in a spherical trap to a delta-like perturbation of quadrupole form. After this perturbation, the shape of the gas shows a damped oscillation. At low temperatures, this oscillation is just the hydrodynamic quadrupole mode which is damped by its coupling to the normal component. With increasing temperatures,

the extension of the normal component increases, and, as a consequence, the normal component can perform its own quadrupole oscillation. Since the frequency of the quadrupole mode in the normal collisionless Fermi gas is higher than that of the hydrodynamic mode, this leads to a two-peak structure in the response function. As the temperature approaches T_c, the strength of the hydrodynamic mode disappears and only the normal mode survives.

The next step will be to apply the method presented here to more realistic cases, namely to the axial and radial breathing modes of a gas in a cigar-shaped trap containing a larger number of particles. In fact, the deformation and the large particle number do not pose a big problem, which is one of the main advantages of the present method as compared with quantum mechanical QRPA calculations. Another possible application of the method is to study the dynamics of a vortex, where already the equilibrium situation is characterized by a non-vanishing phase of the order parameter.

However, there are still a number of unsolved problems and possible improvements of the method. First of all, the collision term [9] should be included, which is an additional source of damping of the collective oscillations. As mentioned in the introduction, the possibility to include collisions is an important advantage of the present method as compared with the QRPA, where collision effects cannot be taken into account since this would necessitate to include four-quasiparticle excitations. Second, from a fundamental point of view, the fact that the continuity equation is only approximately fulfilled is of course unsatisfactory and one should think about another numerical method for solving the continuity equation. Finally, one might ask the question how the present theory can be extended to the strongly interacting regime. Unfortunately, this question is up to now completely open, since in this regime thermal fluctuations of the order parameter, which are not contained in the BdG equations, play a crucial role (see, e.g., Ref. [26]).

[1] M. Bartenstein, A. Altmeyer, S. Riedl, S. Jochim, C. Chin, J. Hecker Denschlag, and R. Grimm, Phys. Rev. Lett. **92**, 203201 (2004); A. Altmeyer, S. Riedl, C. Kohstall, M. Wright, R. Geursen, M. Bartenstein, C. Chin, J. Hecker Denschlag, and R. Grimm, cond-mat/0609390 (2006); A. Altmeyer, S. Riedl, C. Kohstall, M.J. Wright, J. Hecker Denschlag, and R. Grimm, e-print cond-mat/0611285 (2006).

[2] J. Kinast, S.L. Hemmer, M.E. Gehm, A. Turlapov, and

J.E. Thomas, Phys. Rev. Lett. **92**, 150402 (2004); J. Kinast, A. Turlapov, and J.E. Thomas, Phys. Rev. A **70**, 051401(R) (2004).

[3] M. Urban, Phys. Rev. A **71**, 033611 (2005).

[4] E. Taylor and A. Griffin, Phys. Rev. A **72**, 053630 (2005).

[5] G.M. Bruun and B.R. Mottelson, Phys. Rev. Lett. **87**, 270403 (2001); G.M. Bruun, Phys. Rev. Lett. **89**, 263002 (2002).

[6] M. Grasso, E. Khan, and M. Urban, Phys. Rev. A **72**,

043617 (2005).

[7] O. Betbeder-Matibet and P. Nozières, Ann. Phys. (N.Y.) **51**, 392 (1969).

[8] J.W. Serene and D. Rainer, Phys. Rep. **101**, 221 (1983).

[9] D. Vollhardt and P. Wölfle, *The Superfluid Phases of Helium 3* (Taylor & Francis, London, 1990)

[10] M. Urban and P. Schuck, Phys. Rev. A **73**, 013621 (2006).

[11] G.F. Bertsch and S. Das Gupta, Phys. Rep. **160**, 190 (1988).

[12] F. Toschi, P. Vignolo, S. Succi, and M.P. Tosi, Phys. Rev. A **67**, 041605(R) (2003); F. Toschi, P. Capuzzi, S. Succi, P. Vignolo, and M.P. Tosi, J. Phys. B **37**, S91 (2004).

[13] T. Maruyama, H. Yabu, T. Suzuki, Phys. Rev. A **72**, 013609 (2005).

[14] P. Ring and P. Schuck, *The Nuclear Many-Body Problem* (Springer-Verlag, Berlin 1980),

[15] A.L. Fetter and J.D. Walecka, *Quantum Theory of Many-Particle Systems*, (McGraw-Hill, New York 1971).

[16] M. Houbiers, R. Ferwerda, H.T.C. Stoof, W.I. McAlexander, C.A. Sackett, and R.G. Hulet, Phys. Rev. A **56**, 4864 (1997).

[17] M. Grasso and M. Urban, Phys. Rev. A **68**, 033610 (2003).

[18] M.A. Baranov and D.S. Petrov, Phys. Rev. A **58**, R801 (1998).

[19] G. Bruun, Y. Castin, R. Dum, and K. Burnett, Eur. Phys. J. D **7**, 433 (1999).

[20] G.M. Bruun and H. Heiselberg, Phys. Rev. A **65**, 053407 (2002).

[21] C. Bruder and Y. Imry, Phys. Rev. Lett. **80**, 5782 (1998).

[22] G.M. Bruun and C.W. Clark, Phys. Rev. Lett. **83**, 5415 (1999).

[23] M.A. Baranov and D.S. Petrov, Phys. Rev. A **62**, 041601(R) (2000).

[24] M. Cozzini and S. Stringari, Phys. Rev. Lett. **91**, 070401 (2003).

[25] L. Vichi and S. Stringari, Phys. Rev. A **60**, 4734 (1999); C. Menotti, P. Pedri, and S. Stringari, Phys. Rev. Lett. **89**, 250402 (2002).

[26] A. Perali, P. Pieri, L. Pisani, and G.C. Strinati, Phys. Rev. Lett. **92**, 220404 (2004).

[27] There are some typos in Ref. [10] which we wish to correct here: In Eq. (33), Δ should be replaced by $\tilde{\Delta}$. In Eq. (34b), $\dot{\varrho}_{ev}$ should be replaced by $\dot{\nu}_{ev}$. In Eq. (61), $\Delta_{1\nu}(\mathbf{r})$ should be replaced by $-\Delta_{1\nu}(\mathbf{r})$. In addition, we point out that $\tilde{\Delta}_1 = 0$ if $\Delta_0 = 0$, which is not evident from Eq. (61) but can be derived from Eq. (54).